

Substrate Binding and Active Site Residues in RNases E and G

ROLE OF THE 5'-SENSOR^{*[5]}

Received for publication, September 5, 2009. Published, JBC Papers in Press, September 24, 2009. DOI 10.1074/jbc.M109.063263

Stephen M. Garrey, Michaela Blech, Jenna L. Riffell, Janet S. Hankins, Leigh M. Stickney, Melinda Diver, Ying-Han Roger Hsu, Vitharani Kunanithy, and George A. Mackie¹

From the Department of Biochemistry and Molecular Biology, The University of British Columbia Life Sciences Centre, Vancouver, British Columbia V6T 1Z3, Canada

The paralogous endoribonucleases, RNase E and RNase G, play major roles in intracellular RNA metabolism in *Escherichia coli* and related organisms. To assay the relative importance of the principal RNA binding sites identified by crystallographic analysis, we introduced mutations into the 5'-sensor, the S1 domain, and the Mg⁺²/Mn⁺² binding sites. The effect of such mutations has been measured by assays of activity on several substrates as well as by an assay of RNA binding. RNase E R169Q and the equivalent mutation in RNase G (R171Q) exhibit the strongest reductions in both activity (the k_{cat} decrease ~40- to 100-fold) and RNA binding consistent with a key role for the 5'-sensor. Our analysis also supports a model in which the binding of substrate results in an increase in catalytic efficiency. Although the phosphate sensor plays a key role *in vitro*, it is unexpectedly dispensable *in vivo*. A strain expressing only RNase E R169Q as the sole source of RNase E activity is viable, exhibits a modest reduction in doubling time and colony size, and accumulates immature 5 S rRNA. Our results point to the importance of alternative RNA binding sites in RNase E and to alternative pathways of RNA recognition.

The RNase E/G family of bacterial endoribonucleases is widely distributed among bacteria (1). Both RNase E and RNase G are expressed in *Escherichia coli*. RNase E was first characterized as an essential processing enzyme required for the maturation of 5 S rRNA² (2, 3). It is now known also to be involved in processing the 5'-spacer region of 16 S rRNA (4), most tRNA precursors (5, 6), transfer messenger RNA (7), and in the metabolism of many small regulatory RNAs (8, 9). It is also responsible for catalyzing the initial cleavage in the degradation of most mRNAs (10, 11). Furthermore, RNase E is part of a larger complex, the RNA degradosome (12–14). In contrast, RNase G appears to play a more limited role in RNA metabolism. It is responsible for the formation of the mature 5' terminus of 16 S rRNA (4, 15) and participates in the degradation of a limited set of mRNAs (16, 17). It is not essential, however. Although both enzymes prefer single-stranded substrates, neither displays stringent sequence specificity (18–20). However,

both enzymes are 5'-end-dependent; *i.e.* their activity is stimulated, both *in vivo* and *in vitro* by a 5'-monophosphorylated terminus on their substrates (21–26). To explain this observation, it was postulated that a 5'-phosphate binding pocket exists on the surface of these enzymes (24). This idea has been substantially verified by the crystal structure of the catalytic domain of RNase E in complex with a substrate analog (27). These authors showed that RNase E contains a 5'-sensor domain that can interact specifically with a 5'-monophosphorylated substrate via contacts with Gly-124, Val-128, Arg-169, and Thr-170 (27).

Several investigations have identified potential RNA binding surfaces on RNase E in addition to the 5'-sensor, including an arginine-rich region (28–30) and the S1 domain (31, 32). In addition, the active (catalytic) site itself must contribute to substrate binding. The arginine-rich region, however, lies outside the minimal N-terminal domain of RNase E that is sufficient for enzymatic activity (28–30). Several residues in the S1 domain could contribute to RNA binding, but only three, Phe-57, Phe-67, and Lys-112 provide obvious contacts to the substrate (27). Thus, it is not clear to what extent the 5'-sensor contributes to substrate binding. Indeed, it has been suggested that interaction of RNase E or G with a 5'-monophosphorylated substrate increases these enzymes' V_{max} , effectively providing activation of these enzymes (25). Because a crystal structure was not available at the time this work was initiated, we examined instead the role of two types of conserved amino acid residue lying between the S1 domain and residue 400 in RNases E and G. In view of the known requirement of RNase E for transition metal ions (3), we tested whether any of five conserved acidic residues that might chelate Mg⁺² or Mn⁺² would be required for activity or RNA binding. Likewise, we mutated several conserved arginine residues that might be expected to interact with the phosphate backbone of a substrate. We found that the impact of such mutations was generally more severe in RNase G than in RNase E. Quantitative analysis of our data in light of the crystal structure of the N-terminal catalytic domain of RNase E (27) shows that the 5'-phosphate sensor plays a dominant role in substrate binding *in vitro* yet is not essential for survival *in vivo*.

EXPERIMENTAL PROCEDURES

Strains—*E. coli* K12 strain SK9714 (*thyA715*, 8-, *rph-1*, *srlD300::Tn10*, *recA56*, *rne*)1018::*bla*/pSBK1 [Cm^R , rne^+] and plasmid pQLK26 (K_m^R , rne^+) (33) were obtained from Dr. Sidney Kushner, University of Georgia. The host strain for mutagenesis was *E. coli* DH5⁺ (obtained from Invitrogen). The

* This work was supported by Grant MOP-5396 from the Canadian Institutes of Health Research.

[5] The on-line version of this article (available at <http://www.jbc.org>) contains supplemental Figs. S1 and S2 and Tables 1–3.

¹ To whom correspondence should be addressed: Life Sciences Centre, 2350 Health Sciences Mall, Vancouver, British Columbia V6T 1Z3, Canada. Tel.: 604-822-5943; Fax: 604-822-5227; E-mail: gamackie@interchange.ubc.ca.

² The abbreviations used are: rRNA, ribosomal RNA; WT, wild type.

Role of the 5'-Sensor in RNase E/G

host for enzyme overexpression was *E. coli* BL21(DE3) originally obtained from Novagen.

The plasmid pQLK26 was modified by replacing its ~6-kbp insert containing *rne* with a shortened 3881-bp fragment amplified from pQLK26 to form pSG-Rne (see [supplemental Fig. S1, step 1](#), and [supplemental Table 1](#)). The replacement insert contains 600 nucleotides upstream of the *rne* start codon, the entire coding sequence, and 101 nucleotides downstream from the *rne* stop codon. All three *rne* promoters and its transcriptional terminator are included within the 3.8-kbp insert. The empty vector lacks this insert and only contains the backbone from pQLK26 with a single SalI site (this is equivalent to pWSK129 in Ref. 33). To facilitate the construction of mutations in pSG-Rne, the 3.8-kbp insert was further subcloned into pUC19 (see [supplemental Fig. S1, step 2](#)). Appropriate fragments containing a mutation of interest were reassembled in pWSK129 to generate a full-length, mutant *rne* construct (see [supplemental Fig. S1, step 4](#)).

Plasmid displacement from strain SK9714 was measured as follows. Approximately 10^9 competent SK9714 in 0.06 ml were transformed with derivatives of pSG-Rne, allowed to recover in 1.0 ml of LB medium, then diluted 200-fold in LB containing thymidine, kanamycin, tetracycline, and carbenicillin (20 mg/liter each) and allowed to grow to saturation. The saturated culture was diluted 1000-fold into fresh medium also containing selective antibiotics and grown to saturation at 37 °C. Portions of this culture were spread on LB agar plates containing thymidine, kanamycin, tetracycline, and carbenicillin (20 mg/liter each). Colonies were picked onto fresh plates containing thymidine, tetracycline, carbenicillin, and either kanamycin or chloramphenicol. Plasmid displacement was measured as the fraction of kanamycin-resistant colonies that had lost resistance to 20 mg/ml chloramphenicol.

Construction of Rne or Rng Mutants and Purification of Mutant Enzymes—Plasmid pSG-Rne1–529 was constructed in the pET24b (Novagen) backbone between the NdeI and XhoI sites using appropriate PCR primers (see [supplemental materials](#)) to amplify DNA corresponding to amino acid residues 1–529 from *E. coli* DNA. The resultant construct will encode a C-terminal hexahistidine tag. Additional mutants were made as described below with the primers listed in [supplementary materials](#).

Plasmid pDB1, based on pET24b, encodes RNase G with six additional N-terminal histidine residues (34) and was the basis for all further constructions involving RNase G. Mutagenesis was performed using the Stratagene QuikChange® kit. Oligonucleotides used for mutagenesis are listed in [supplemental Table 3](#). Putative mutant plasmids were checked for the desired change by DNA sequence analysis.

His₆-RNase E (1–529), His₆-RNase G, and derived mutants were purified as described (34). In brief, cell pellets from 1 liter of induced cultures grown to saturation at 20 °C were harvested and lysed in a French pressure cell (Amino). A cleared lysate was passed through a column packed with Talon resin (Clontech). Fractions eluted with >50 mM imidazole were pooled, supplemented with 6 mM 2-mercaptoethanol, and subjected to further chromatography on a column of Source Q (Amersham Biosciences). Fractions containing the desired RNase were

pooled, made 1 mM in dithiothreitol, and quantified prior to further characterization.

RNase Assays—Three RNA substrates were used in assays of activity. The first was Ribo-8 (5'-ACAGUAUUUdG), a derivative of BR10 (20) containing a 3'-deoxy-G residue. The other substrates were BR14-FD (25; see Fig. 2A below) and BR13-3'-fluorescein (26). Assays using Ribo-8 contained 50 nM 5'-³²P-Ribo-8 and RNase G or its mutants in 25 mM Tris-HCl, pH 7.8, 5 mM MgCl₂, 30 mM KCl, 1 mM dithiothreitol, and 5% glycerol. Incubations were initiated by addition of enzyme (8 nM for wild type; see "Effects of Mutation on Enzyme Activity" under "Results"). Samples were removed at timed intervals, denatured in buffered 90% formamide, and boiled for 45 s. Products were separated by electrophoresis on a 15% polyacrylamide gel (29:1 acrylamide:bis acrylamide) containing 8 M urea and detected by phosphorimaging.

The fluorescent substrates, 5'-P-BR14-FD (25) and 5'-P-BR13F (26), were synthesized by the University Core DNA Services at the University of Calgary. Assays were performed at 30 °C in a buffer containing 25 mM Tris-HCl, pH 7.6, 10 mM MgCl₂, 30 mM NaCl, 1 mM dithiothreitol, and 5% (v/v) glycerol. For BR14FD, fluorescence at 517 nm was monitored on a Cary Eclipse fluorescence spectrophotometer using excitation at 495 nm. Initial rates were determined by monitoring the increase of fluorescence over the first 5 min following addition of enzyme (*i.e.* in the linear range). Measurements of initial rates for a given substrate concentration were repeated at least three times, and the average was determined. For assays with BR13F, portions of the assay were withdrawn, quenched in 3 volumes of buffered 90% formamide, and treated as for BR13 above, except that wet gels were scanned for fluorescence using a Typhoon phosphorimaging device. Kinetic constants were extracted from the data using an Eadie-Hofstee plot.

RNA Binding Assays—We adapted the double filter assay of Wong and Lohman (35) to measure the binding of 5'-³²P-Ribo-8 to RNase G. Briefly, incubations containing 20 nM RNA oligonucleotide and from 100 nM to 4 mM RNase G were assembled on ice in FAB buffer (20 mM PIPES, 50 mM NaCl, 0.5 mM EDTA, 0.5 mM dithiothreitol, 20 μg/ml acetylated bovine serum albumin (New England Biolabs), pH 6.5). Samples were applied to individual wells in a Bio-Rad 96 well dot-blot apparatus containing a Bio-Rad nitrocellulose membrane over an Amersham Biosciences Hybond-NX nylon membrane, both previously washed with 1× FAB at room temperature. The samples were incubated for 5 min at ambient temperature before being drawn through the membranes with a gentle vacuum and washed with 100 ml of 1× FAB. Membranes were allowed to dry under suction for 5 min and were then exposed to a phosphor storage screen.

Northern Blotting—Total RNA was extracted from exponential cultures grown in LB medium supplemented with 50 μg/ml thymidine and appropriate antibiotics. Samples (3 μg) were dissolved in 8 μl of buffered 80% formamide, separated in a 5% polyacrylamide gel containing 8 M urea in Tris borate-EDTA buffer, and electrophoretically transferred to Hybond NX. Hybridization was performed at 35.5 °C as described before (42) using a 5'-³²P-labeled oligonucleotide complementary to 5 S RNA (5'-CGTTTCACTTCTGAGTTCGGC).

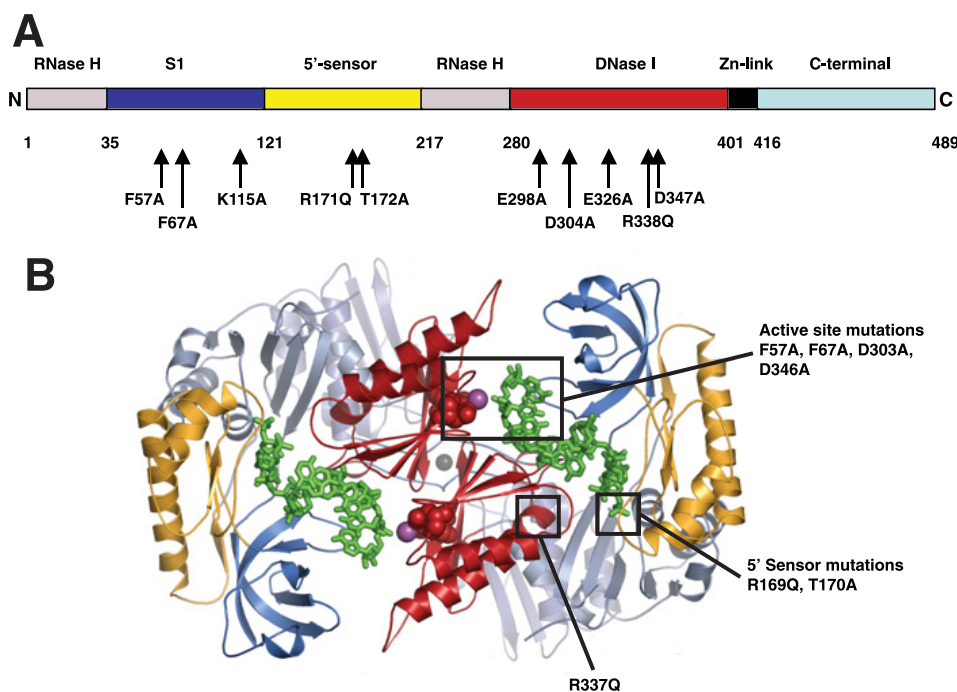


FIGURE 1. *A*, schematic map of RNase G. This *linear map* of RNase G shows the domains inferred from alignment against RNase E. The boundaries are given by the residue numbers below the *linear map* and correspond to those in RNase E (27). The positions of mutations in RNase G created in this work are noted below the map. *B*, structure of the N terminus of RNase E. The *ribbon diagram* was provided by Dr. Ben Luisi and shows the N-terminal region of two monomers of RNase E (27). The positions of substrates (in green) prior to cleavage and the positions of some of the mutations created in this study, are indicated using *space-filling atoms*. Domains are similarly colored in both *A* and *B*.

RESULTS

Identification and Mutation of Conserved Residues in RNase G—Our goal was the clarification of the role of different potential RNA binding domains in RNase E on this enzyme's activity. However, to avoid some of the complexities of RNase E, including its association with other proteins (12–14) and membranes (36) as well as potential RNA binding sites outside the catalytic domain (28, 29), we initially used RNase G as a surrogate. This enzyme displays 5'-end dependence (22–23), like RNase E (21), and can be assayed against the same substrates (25). We postulated that residues playing important functions in catalysis and substrate binding would be highly conserved in both RNase E and RNase G. To this end, we constructed an alignment of the members of the RNase E and RNase G family similar to published alignments (1, 27). In particular, we identified Glu-298, Asp-304, Glu-326, Asp-347, and Asp-350 in RNase G (Glu-297, Asp-303, Glu-325, Asp-346, and Asp-349, respectively, in RNase E) as conserved acidic residues that could play a role in metal ion chelation. Likewise, Arg-171 and Arg-338 (Arg-169 and Arg-337, respectively, in RNase E) are highly conserved basic residues that could interact with backbone phosphates. Each of these residues was mutated independently to Ala or Gln, and the resultant mutant proteins were expressed, purified, and characterized. Fig. 1*A* summarizes the mutations used in this study and indicates their location in the presumed domain structure of RNase G. A typical purification of a mutant enzyme, RNase G R171Q, is shown in the [supplemental material](#). The enzyme was substantially pure after immobilized metal ion chromatography and was essentially

homogeneous after ion-exchange chromatography (see [supplemental Fig. S2B](#)). In several cases, mutant proteins were further characterized by mass spectrometry. Interestingly, for RNase G D347A and D350A, the observed masses of 56,420 and 56,432, respectively, correspond to the expected loss of mass associated with a change from Asp to Ala, but with the retention of the *N*-formyl group at the *N* terminus (expected mass, 56,433).

We also examined several physical properties of some of the mutant enzymes. The mid-point unfolding temperature (T_m) was determined for several mutants using CD (34). Generally, the mutants tested displayed a T_m equal to that of His₆-RNase G (50.3 °C (34)). RNase G D350A, however, displayed a somewhat lower T_m (approx 47 °C). Nonetheless, this mutant enzyme cosedimented with His₆-RNase G implying that it was still capable of forming dimers (data not shown).

Effects of Mutation on Enzyme Activity

Many of the mutant enzymes were initially assayed on a 519-nucleotide substrate, which mimics the RNase III-processed pre-16 S rRNA (34). Although this assay is rather insensitive, several mutants, including RNase G R171Q, D304A, and D347A exhibited detectable losses in activity (>50%; data not shown). More informative data were obtained by assaying each of the mutant enzymes against 5'-³²P-Ribo-8 (Table 1). Although wild-type RNase G could be assayed at limiting enzyme concentrations, most of the mutants had to be assayed in enzyme excess. Nonetheless, RNase G R171Q (5'-sensor domain) and D304A (active site) were virtually inactive. Modest levels of activity could be observed with RNase G F67A and K115A (both in the S1 domain), and R171H and R338Q, especially at high enzyme concentrations. The remaining mutants, including RNase G V131I, E298A, E326A, D347A, and D350A, retained significant levels of activity against this substrate (Table 1). Although Glu-298 and Glu-326 are conserved, they appear not to be required for activity under the conditions tested and were not characterized further. As a control for the validity of the assay, in particular for its sensitivity to the status of the substrate's 5'-end, we repeated several assays with 5'-hydroxyl, 3'-³²pCp-BR10 as a substrate to determine the fraction of activity that was 5'-end-independent. His₆-RNase G displayed only ≤6% as much activity on this 5'-OH substrate as on 5'-³²P-Ribo-8 (data not shown). Moreover, the mutants tested, including R171Q and R338Q, were virtually inactive against this 5'-OH substrate (data not shown).

To obtain kinetic parameters, we assayed many of the mutant enzymes against BR14FD, a fluorescent oligoribonucleotide

Role of the 5'-Sensor in RNase E/G

substrate developed by Jiang and Belasco (25). Representative time courses and Eadie-Hofstee plots are shown in Fig. 2, whereas the kinetic data are summarized in Table 1. In general,

TABLE 1
Relative activities and affinities of RNase G point mutants

Enzyme	Ribo-8 ^a	Kinetic constants ^b		Binding, K_d app ^c
		K_m	k_{cat}	
	% activity	nM	min ⁻¹	nM
WT (His ₆)	100	70	1.4	190
F57A	ND ^d	210	0.01	1200
F67A	≤5	460	0.044	900
K115A	≤5	110	0.046	1000
V131I	50	ND	ND	ND
R171Q	≤1	≥1000 ^e	0.015 ^e	>5000
R171H	≤10	ND	ND	ND
E298A	100	ND	ND	ND
D304A	≤2	330	0.014	840
E326A	100	ND	ND	ND
R338Q	15	210	0.011	>1000
D347A	40	300	0.046	670
D350A	8	230	0.80	540

^a Activities were measured with 5'-³²P-Ribo-8 and are reported as apparent initial rates of formation of 5-nucleotide product expressed as a percentage of the rate measured for His₆-RNase G. Most of the mutants were assayed in enzyme excess to obtain measurable rates while wild type was assayed in substrate excess. Values are the average of duplicates.

^b Except as noted in footnote *e* below, kinetic constants were estimated from Eadie-Hofstee plots of data generated from assays using 5'-P-BR14FD as substrate (see "Experimental Procedures"). Each enzyme was assayed in triplicate, and initial rates for each concentration of substrate were averaged. The averaged values were then used to obtain slopes and intercepts.

^c Binding data, usually in triplicate, using ³²P-Ribo-8 as ligand were obtained from the double filter method (see "Experimental Procedures") and are reported as apparent K_d values.

^d ND, not determined.

^e Because BR14FD could not be used at concentrations > 800 nM, we employed an in-gel assay with 5'-P-BR13F containing a 3'-fluorescein modification to obtain kinetic parameters for R171Q (26; see "Experimental Procedures").

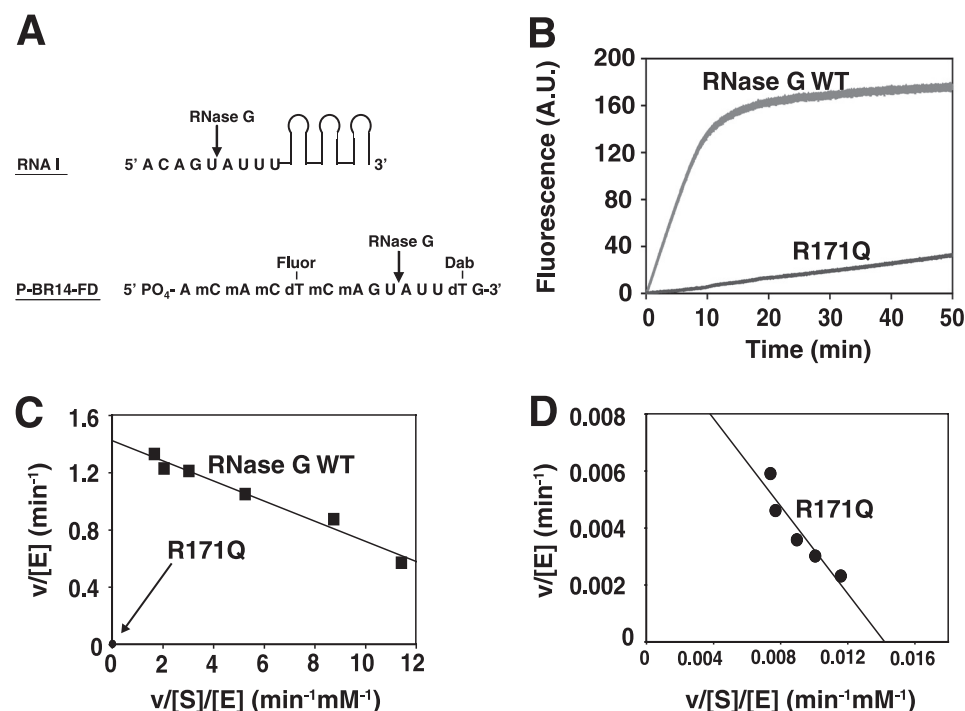


FIGURE 2. Fluorescence assay of RNase G. *A*, shows a schematic of RNA 1, a 108-nucleotide regulatory RNA that is a model substrate for RNase E. The major cleavage site is denoted by the vertical arrow. BR14FD, a synthetic fluorescent substrate for RNase E or G is based on the 5'-end of RNA 1 (25). *B*, time course showing the increase in fluorescence as BR14FD is cleaved under conditions described under "Experimental Procedures." *C*, Eadie-Hofstee plot of initial rates as a function of concentration of BR14FD. The data for RNase G R171Q are compressed in this graph. *D*, expansion of the data in *C* to show the Eadie-Hofstee plot for RNase G R171Q.

the results obtained with this assay are qualitatively similar to the data obtained with Ribo-8. The fluorescence assay is, however, far more sensitive and can be conducted at limiting enzyme concentrations. WT (His₆) RNase G exhibited a K_m of 70 nM and a k_{cat} of 1.4 min⁻¹ (Fig. 2, *C* and *D*, and Table 1). These values are similar to those reported by Jiang and Belasco: 230 nM and 2.1 min⁻¹ (25). They also compare favorably to 120 nM and 3.0 min⁻¹, respectively, reported by Jourdan and McDowall (26) using a somewhat different fluorescence assay. To verify the 5'-end dependence of RNase G under these conditions (22, 23, 25), wild-type RNase G was assayed against 5'-OH-BR14. With this substrate, the K_m increased to 570 nM, and the k_{cat} fell to 0.03 min⁻¹. This result differs from that reported by Jiang and Belasco (25) who found that the state of phosphorylation of BR14 did not affect K_m but only k_{cat} . In this regard, our results more closely agree with those of Jourdan and McDowall (26).

The use of fluorescent substrates permitted an objective comparison of the mutants. The most striking of these is RNase G R171Q for which the k_{cat} drops by almost 100-fold while the K_m increases ~14-fold (Fig. 2*D* and Table 1). This finding points to the key role in the recognition of some substrates that is played by the phosphate binding pocket in RNase G (see "Discussion"). Interestingly, mutations in three residues in the S1 domain, which line the RNA binding channel, Phe-57, Phe-67, and Lys-115 (27), also affect both kinetic parameters, but not as severely. The K_m increases 3- to 7-fold while the catalytic efficiency, k_{cat} , falls 30- to 140-fold. Among the putative metal ion chelating residues, mutations in either Asp-304 or Asp-347 affect both K_m and k_{cat} , with D304A being the more severe mutation. In contrast, D350A exerts only a modest effect on K_m and little effect on k_{cat} (see Table 1). The strong effects of mutations on Asp-304 and Asp-347 agree with the findings of Callaghan *et al.* (27) for the N-terminal domain of RNase E (see below).

RNA Binding by Mutant RNase G Enzymes—We employed a double filter assay (35) to determine the relative affinities of His₆-RNase G and its derivatives for 5'-³²P-Ribo-8 (see "Experimental Procedures"). The main challenge was avoidance of contamination by Mg⁺² ions and the resultant destruction of the ligand by cleavage. Typical binding isotherms are shown in Fig. 3, and the data are summarized in Table 1. Wild-type RNase G displayed an apparent K_d of 190 nM. This value is close to the K_d of 162 nM reported by Jourdan and McDowall (26) who used fluorescence anisotropy to assess RNA binding to a 2'-*O*-methyl substrate. In contrast, R171Q exhibited very little

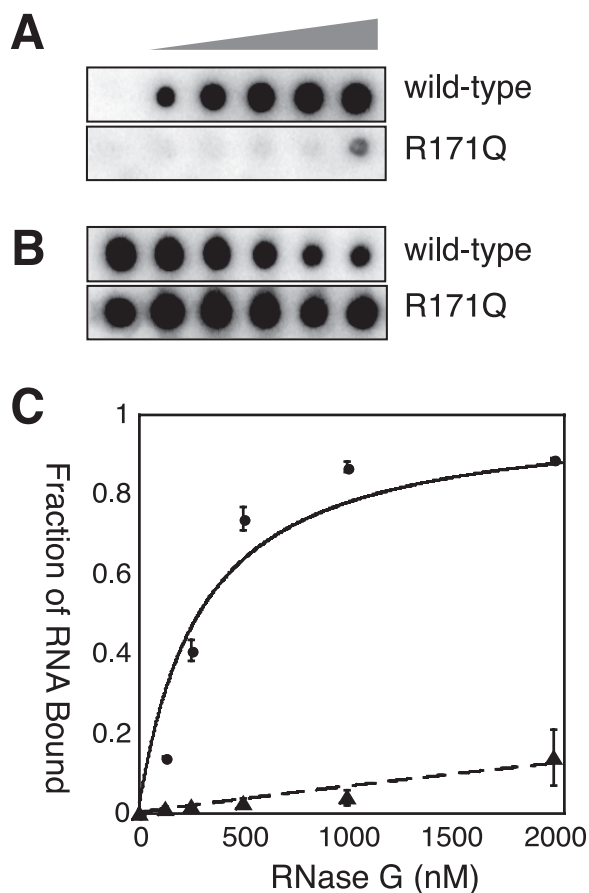


FIGURE 3. Double filter assay of RNA binding by RNase G. The assay of Wong and Lohman (35) was adapted for RNase G as described under “Experimental Procedures.” A typical set of data is shown. The *left hand column* in each *panel* contained no added protein. Protein concentrations ranged from 125 to 2000 nM from *left to right*. *A*, nitrocellulose filter (retaining RNA-protein complexes); *B*, nylon filter with free RNA. The RNase G preparations assayed for binding are listed in the *right margin*. *C*, fraction of RNA bound as a function of protein concentration for WT RNase G (●) and RNase G R171Q (▲).

binding to this RNA ligand at the protein concentrations tested (Fig. 3C and Table 1). The F57A, F67A, and K115A mutations in the S1 domain also resulted in lowered RNA binding with apparent K_d values of 900–1200 nM, respectively, or 5-fold more than wild type. Interestingly, mutations in the metal binding site, including D304A and D347A, resulted in partial loss of binding to Ribo-8 and elevated K_d values. Nonetheless, the data show that the most severe effect on RNA binding, a >25-fold increase in K_d , is exerted by R171Q. In support of this finding, we tested the binding of 3'-fluorescein-labeled BR13, with or without a 5'-monophosphate, to wild-type RNase G. Binding of 5'-OH-BR13F was much weaker than that of BR13-5'-monophosphate and did not reach 50% at the highest protein concentration tested.

Effect of Selected Mutations on RNase E—To test the implied assumption that the effect of mutations in RNase G could be extrapolated to RNase E, we reconstructed some of the most severe alleles of RNase G in a derivative of RNase E spanning residues 1–529 (*i.e.* the catalytic domain used for crystallographic analysis (27)). Mutant proteins were expressed and purified as described for RNase G (see “Experimental Procedures”), and then assayed on BR14FD. These data are summa-

TABLE 2
 Relative activities of RNase E point mutants

Enzyme ^a	Kinetic constants ^b	
	K_m nM	k_{cat} min ⁻¹
WT	33	11
WT ^c	5100	0.95
F57A	120	1.9
F67A	320	1.1
R169Q	350	0.28
D303A	38	0.008
D346A	77	0.007

^a In all cases, the enzyme includes residues 1–529 of RNase E.

^b Except where noted, kinetic constants were estimated from Eadie-Hofstee plots of data generated with 5'-P-BR14FD as substrate (see “Experimental Procedures”). Rates for each substrate concentration were determined at least in triplicate, then averaged prior to plotting.

^c Data on this line were obtained with 5'-OH-BR14FD as substrate (see “Experimental Procedures”).

rized in Table 2. Several salient observations emerge by comparison to the data in Table 1. First, RNase E is more active than RNase G (*i.e.* lower K_m and higher k_{cat}). This differs from the findings of Jiang and Belasco (25) and may reflect the fact the RNase E construct used by these authors was shorter than the one employed here. Second, mutations in the S1 domain of RNase E (F57A and F67A) exert modest increases in K_m (4- to 10-fold) and decreases in k_{cat} (6- to 12-fold). The corresponding mutations in RNase G, however, resulted in 30- to 100-fold reductions in k_{cat} (Table 1). Third, the R169Q mutation in RNase E (5'-sensor domain) increases the K_m 10-fold and decreases the k_{cat} almost 40-fold. The change in k_{cat} , in particular, is less severe than observed in the corresponding mutation in RNase G (*i.e.* R171Q). As a control, we tested the 5'-end dependence of RNase E 1–529. Dephosphorylating the substrate led to a 36-fold increase in K_m and a 32-fold decrease in k_{cat} consistent with the effects of the R169Q mutation (see Table 2). Finally, the mutation D303A reduced k_{cat} by 1000-fold, essentially eliminating activity as did D304A in RNase G (Table 1). We were unable to measure the affinity of RNase E 1–529 or any of its derived mutants for Ribo-8 by the double filter method, because binding was too weak and did not reach saturation.

Effect of Mutations in RNA Binding Residues of RNase E in Vivo—Because RNase G is not essential in *E. coli* under normal laboratory conditions we instead determined the phenotype of mutations in the corresponding residues in RNase E, because the latter enzyme is essential for viability (10, 33). Mutations were constructed in the *rne* gene carried on pSG-Rne, a derivative of pQLK26 (K_m^R), a low copy plasmid capable of complementing *rne*Δ1018::bla, an otherwise lethal deletion of the chromosomal *rne* gene (33). Each such construct was tested for its ability to displace a wild-type plasmid, pSBK1 (*rne*+, Cm^R), from strain SK9714, which requires a functional *rne* gene supplied in *trans* for survival. Data for such experiments are shown in Table 3. The mutants tested fall into two clear classes. The first fails to displace pSBK1 and includes F67A, D303A, D346A, and R337E. Phe-67 interacts with the RNA substrate in the S1 domain close to the catalytic site, while Asp-303 and Asp-346 are believed to chelate an essential Mg⁺² ion and participate in catalysis (27). Our data support this view and demonstrate that

Role of the 5'-Sensor in RNase E/G

TABLE 3
Complementation of a lethal *rne* deletion by *rne* mutants

Mutation	Plasmid ^a	Percent displaced ^b
		%
WT	pSG-Rne	76 ± 4.1
F57A	pSG-Rne F57A	93 ± 1.0
F67A	pSG-Rne F67A	0
R169Q	pSG-Rne R169Q	47 ± 5.0 ^c
T170A	pSG-Rne T170A	89 ± 2.3
D303A	pSG-Rne D303A	0
R337E	pSG-Rne R337E	0
R337Q	pSG-Rne R337Q	92 ± 1.2
D346A	pSG-Rne D346A	0

^a All complementing plasmids were constructed in the backbone from pWSK129 (see "Experimental Procedures" and supplemental Fig. S1).

^b The fraction displaced is recorded as the fraction of colonies that have acquired resistance to kanamycin via the mutant plasmid with concomitant loss of resistance to chloramphenicol conferred by pSBK1 after >20 doublings (see "Experimental Procedures").

^c Colonies that were resistant to kanamycin but sensitive to chloramphenicol were noticeably smaller than those that retained pSBK1 (see also Fig. 4).

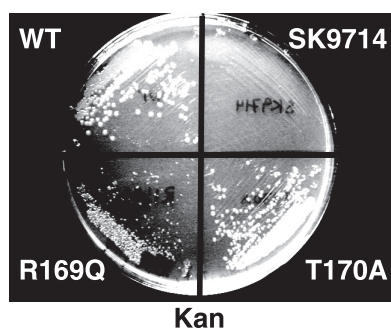


FIGURE 4. Colony Size of SK9714 transformed with different plasmids. Samples of cultures of SK9714 (33) transformed with plasmids of interest (see Table 2) were streaked on plates containing LB, thymidine, carbenicillin, and kanamycin.

these residues are essential for RNase E. The deleterious effect of R337E is most likely due to the charge reversal caused by this substitution because R337Q displays almost no phenotype (Table 3). The second class of mutants was able to displace pSBK1 at significant frequencies (Table 3). These mutants, including F57A, R169Q, and T170A, affect residues involved in contacting RNA in the S1 domain (Phe-57) or phosphate binding pocket (27). Although R169Q was able to displace pSBK1 at a significant frequency, the resultant colonies were noticeably smaller (Fig. 4). Transformants of SK9714 containing pSG-Rne-R169Q grew with a doubling time of 32.3 min in rich medium. In contrast, SK9714 containing pSG-Rne (WT) grew significantly more quickly under the same conditions with a doubling time of 24.5 min. Strains transformed with pSG-Rne T170A, which showed no phenotype, also grew well, with a doubling time of 27 min.

We further characterized the three mutants able to displace WT pSG-Rne by examining the accumulation of 5 S RNA. For comparison, we also included the well known temperature-sensitive *rne-1* allele. Fig. 5 shows that precursors to 5 S RNA accumulate at non-permissive temperature in the *rne-1* strain, SK5665 (compare lane 2 to lane 1), as expected. A strain containing pSG-Rne R169Q as its only source of RNase E exhibits a pattern of precursor accumulation that is qualitatively identical to that of the *rne-1* allele (compare lane 5 to lane 2). In contrast, a strain carrying the T170A allele contains almost no precursors at this exposure (compare lane 6 to lanes 2 and 5), although

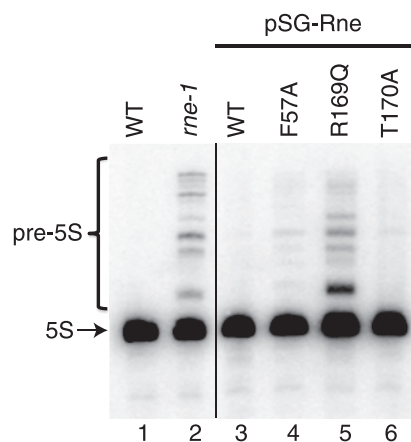


FIGURE 5. Effect of RNase E mutations on stable RNA processing. Total RNA from the following strains was subjected to Northern blotting as described under "Experimental Procedures" using a probe complementary to 5 S rRNA and its precursors: lane 1, MG1693 (WT); lane 2, SK5665 (*rne-1*); lane 3, SK9714/pSG-Rne (WT); lane 4, SK9714/pSG-Rne F57A; lane 5, SK9714/pSG-Rne R169Q; and lane 6, SK9714/pSG-Rne T170A. The position of mature 5 S RNA is shown by the arrow in the left margin.

they are detectable with longer exposures. Interestingly, the F57A allele (lane 4) also accumulates some precursors but to a lesser extent than either *rne-1* or R169Q. Processing of the *hisR* transcript (tRNA^{His}) from the same strains was also tested. Unlike the case above, it was normal in R169Q and T170A, but defective in *rne-1* as expected (6) (data not shown).

DISCUSSION

This investigation was initiated with the goal of using conserved residues identified by bioinformatic means or subsequently, the crystal structure of RNase E (27), to clarify the contribution of potential RNA binding surfaces to the activity of RNases E and G. A major focus was the interaction with the 5'-phosphate of substrates and its mechanism of stimulation of the activity of RNase E and G. The 5'-end dependence of RNase E (21) is a signature property of RNase E and RNase G (22, 23). Interestingly, the unrelated RNase J1 of *Bacillus subtilis* also exhibits a preference of 5'-phosphates (37). At least two mechanisms have been invoked to explain why 5'-monophosphorylated RNAs are preferred by RNases E and G. Jiang and Belasco (25) have presented data that suggest that binding of a monophosphorylated oligonucleotide to RNase E or RNase G stimulates V_{max} up to 30-fold with little effect on K_m . These authors did not measure RNA binding independently of catalysis. In contrast, Jourdan and McDowall (26) reported that the stimulatory effect of a 5'-monophosphate on RNase G is exerted primarily through enhanced substrate binding resulting in a 100-fold improvement in K_m . Our data, using the same substrate as Jiang and Belasco, support the view that the primary effect of a 5'-monophosphorylated substrate is enhanced binding. Neutralization of the positive charge on a key residue in the phosphate binding pocket, Arg-171, resulted in a ~14-fold drop in K_m and a 100-fold decrease in k_{cat} by RNase G. Furthermore, measurement of substrate binding in the absence of catalysis showed that the same mutation caused a 25-fold or greater loss in affinity for substrate. Quantitatively, the loss of affinity for RNA by R171Q is greater than by F57A,

F67A, or K115A, residues in the S1 domain that line the RNA binding channel. The corresponding residues are known to affect the activity of RNase E as assessed by loss of feedback regulation (31). Nonetheless, our data show that binding of a monophosphorylated substrate to RNase E or RNase G also activates the enzyme as proposed (27, 38). Koslover *et al.* have shown that binding of a substrate via its 5-monophosphate residue triggers a significant conformational change in RNase E involving both the 5'-sensor and S1 domains (38). In this regard, interactions between substrate and enzyme remote from the catalytic site are known to contribute to the efficiency of catalysis (39). The large decreases in k_{cat} exhibited by RNase E R169Q and by G R171Q are, in this view, obvious consequences of weak substrate binding.

Based on previous data (31), we anticipated that RNase E F57A might be unable to displace pSBK1 from strain SK9714. Nonetheless, displacement was very efficient. Apparently the reduced activity of RNase E F57A is still sufficient to support growth and results in only modest impairment of 5 S rRNA processing. We presume that requirements for autoregulation (31) differ subtly from those for viability.

The physiological effects of mutations in residues in the phosphate binding pocket of RNase E have not previously been reported. To our surprise, both R169Q and T170A are viable, although the former leads to a slow growth phenotype, small colonies, and significant reduction in the rate of 5 S RNA processing. Conversely, mutations D303A and D346A are inviable, consistent with their proposed role in coordinating a hydrated Mg^{+2} ion that serves as the source of a base in phosphodiester bond cleavage (26, 27). The modest effect of R169Q on RNase E *in vivo* stands in stark contrast to its effects on both RNase E and RNase G *in vitro* (26). This dichotomy suggests that the role of the phosphate sensor is more subtle than initially envisaged. We believe that at least two factors should be considered in explaining this outcome. First it is noteworthy that the most pronounced effects of either monophosphorylation or mutations in the phosphate sensor are detected with oligonucleotides such as BR10 and its derivatives or relatively short substrates (*e.g.* the 9 S RNA precursor to 5 S RNA (246 residues)) (21, 22, 23, 26). Such short substrates may make relatively few contacts with RNase E and thus rely on the phosphate sensor and the S1 domain for binding. Second, at least one additional RNA binding surface is known in full-length RNase E, notably the "arginine-rich region" between residues 610 and 632 (28–30). A comparable region is not found in RNase G. The arginine-rich region may be able to compensate, in part, for deficiencies in 5'-end recognition in R169Q. In this regard, a strain carrying $\Delta rppH$ and thus unable to remove the terminal pyrophosphate from RNAs is viable, although the half-lives of many mRNAs are elevated in this strain (40). We infer, therefore, that internal entry (41, 42) may play a greater role in the action of RNase E, particularly on longer RNAs, than hitherto appreciated. The availability of the viable R169Q mutation will greatly facilitate elucidating the physiological role of the 5'-sensor and investigating possible alternative pathways of substrate recognition.

Acknowledgments—We thank Dr. Sidney Kushner for his gift of strains, Dr. Ken McDowall for sharing data in advance of publication and for providing comments on the ms, and Dr. Ben Luisi for providing a high resolution image of the catalytic domain of RNase E. The fluorometer was provided through a grant from the Canada Foundation for Innovation and the Michael Smith Foundation to the University of British Columbia Laboratory of Molecular Biophysics.

REFERENCES

- Condon, C., and Putzer, H. (2002) *Nucleic Acids Res.* **30**, 5339–5346
- Ghora, B. K., and Apirion, D. (1978) *Cell* **15**, 1055–1066
- Misra, T. K., and Apirion, D. (1979) *J. Biol. Chem.* **254**, 11154–11159
- Li, Z., Pandit, S., and Deutscher, M. P. (1999) *EMBO J.* **18**, 2878–2885
- Li, Z., and Deutscher, M. P. (2002) *RNA* **8**, 97–109
- Ow, M. C., and Kushner, S. R. (2002) *Genes Dev.* **16**, 1102–1115
- Lin-Chao, S., Wei, C. L., and Lin, Y. T. (1999) *Proc. Nat. Acad. Sci. U.S.A.* **96**, 12406–12411
- Carpousis, A. J. (2003) *Genes Dev.* **17**, 2351–2355
- Massé, E., Escoria, F. E., and Gottesman, S. (2003) *Genes Dev.* **17**, 2374–2383
- Coburn, G. A., and Mackie, G. A. (1999) *Prog. Nucleic Acids Res. Mol. Biol.* **62**, 55–108
- Carpousis, A. J. (2007) *Annu. Rev. Microbiol.* **61**, 71–87
- Carpousis, A. J., Van Houwe, G., Ehretsmann, C., and Krisch, H. M. (1994) *Cell* **76**, 889–900
- Miczak, A., Kaberdin, V. R., Jakobsen, J. S., Lin-Chao, S., McDowall, K. J., and von Gabain, A. (1998) *Proc. Natl. Acad. Sci. U.S.A.* **95**, 11637–11642
- Py, B., Higgins, C. F., Krisch, H. M., and Carpousis, A. J. (1996) *Nature* **381**, 169–172
- Wachi, M., Umitsuki, G., Shimizu, M., Takada, A., and Nagai, K. (1999) *Biochem. Biophys. Res. Commun.* **259**, 483–488
- Umitsuki, G., Wachi, M., Takada, A., Hikichi, T., and Nagai, K. (2001) *Genes Cells* **6**, 403–410
- Wachi, M., Kaga, N., Umitsuki, G., Clark, D. P., and Nagai, K. (2001) *Biochem. Biophys. Res. Commun.* **289**, 1301–1306
- Mackie, G. A. (1992) *J. Biol. Chem.* **267**, 1054–1061
- McDowall, K. J., Lin-Chao, S., and Cohen, S. N. (1994) *J. Biol. Chem.* **269**, 10790–10796
- McDowall, K. J., Kaberdin, V. R., Wu, S. W., Cohen, S. N., and Lin-Chao, S. (1995) *Nature* **374**, 287–290
- Mackie, G. A. (1998) *Nature* **395**, 720–723
- Jiang, X., Diwa, A., and Belasco, J. G. (2000) *J. Bacteriol.* **182**, 2468–2475
- Tock, M. R., Walsh, A. P., Carroll, G., and McDowall, K. J. (2000) *J. Biol. Chem.* **275**, 8726–8732
- Spickler, C., Stronge, V., and Mackie, G. A. (2001) *J. Bacteriol.* **183**, 1106–1109
- Jiang, X., and Belasco, J. G. (2004) *Proc. Nat. Acad. Sci. U.S.A.* **101**, 9211–9216
- Jourdan, S. S., and McDowall, K. J. (2008) *Mol. Microbiol.* **67**, 102–115
- Callaghan, A. J., Marcaida, M. J., Stead, J. A., McDowall, K. J., Scott, W. G., and Luisi, B. F. (2005) *Nature* **437**, 1187–1191
- Cormack, R. S., Genereaux, J. L., and Mackie, G. A. (1993) *Proc. Nat. Acad. Sci. U.S.A.* **90**, 9006–9010
- Kaberdin, V. R., Walsh, A. P., Jakobsen, T., McDowall, K. J., and von Gabain, A. (2000) *J. Mol. Biol.* **301**, 257–264
- McDowall, K. J., and Cohen, S. N. (1996) *J. Mol. Biol.* **255**, 349–355
- Diwa, A. A., Jiang, X., Schapira, M., and Belasco, J. G. (2002) *Mol. Microbiol.* **46**, 959–969; erratum (2003) **47**, 1183
- Schubert, M., Edge, R. E., Lario, P., Cook, M. A., Strynadka, N. C., Mackie, G. A., and McIntosh, L. P. (2004) *J. Mol. Biol.* **341**, 37–54
- Ow, M. C., Liu, Q., and Kushner, S. R. (2000) *Mol. Microbiol.* **38**, 854–866
- Briant, D. J., Hankins, J. S., Cook, M. A., and Mackie, G. A. (2003) *Mol. Microbiol.* **50**, 1381–1390
- Wong, I., and Lohman, T. M. (1993) *Proc. Natl. Acad. Sci. U.S.A.* **90**,

Role of the 5'-Sensor in RNase E/G

- 5428–5432
36. Khemici, V., Poljak, L., Luisi, B. F., and Carpousis, A. J. (2008) *Mol. Microbiol.* **70**, 799–813
37. de al Sierra Gallay, I. L., Zig, L., Jamali, A., and Putzer, H. (2008) *Nat. Struct. Mol. Biol.* **15**, 206–212
38. Koslover, D. J., Callaghan, A. J., Marcaida, M. J., Garman, E. F., Martick, M., Scott, W. G., and Luisi, B. F. (2008) *Structure* **16**, 1238–1244
39. Wicki, J., Schloegl, J., Tarling, C. A., and Withers, S. G. (2007) *Biochemistry* **46**, 6996–7005
40. Deana, A., Celesnik, H., and Belasco, J. G. (2008) *Nature* **451**, 355–358
41. Joyce, S. A., and Dreyfus, M. (1998) *J. Mol. Biol.* **282**, 241–254
42. Baker, K. E., and Mackie, G. A. (2003) *Mol. Microbiol.* **47**, 75–88

Supplementary material for

SUBSTRATE BINDING AND ACTIVE SITE RESIDUES IN RNases E AND G: THE ROLE OF THE 5'-SENSOR

Stephen M. Garrey, Michaela Blech, Jenna L. Riffell, Janet S. Hankins, Leigh M. Stickney,
Melinda Diver, Ying-Han Roger Hsu, Vitharani Kunanithy, and George A. Mackie *

From the Department of Biochemistry & Molecular Biology,
The University of British Columbia Life Sciences Centre,
2350 Health Sciences Mall,
Vancouver BC, Canada V6T 1Z3

Running Head: Role of the 5'-sensor in RNase E / G

Address correspondence to: George A. Mackie, Ph.D., Life Sciences Centre, 2350 Health
Sciences Mall, Vancouver BC, Canada V6T 1Z3. Fax: 604-822-5227; Email:
gamackie@interchange.ubc.ca

Legends

SUPPLEMENTARY FIGURE 1. **Construction of plasmids expressing mutant RNase E.** Plasmid pSG-Rne was derived from pQLK26 (1) by replacing the ~6 kb insert (Sall/Sall) spanning the *rne* gene with a shortened 3,881 bp insert (Sall/Sall), amplified from pQLK26 (Step 1; see Table 1 for primers). The new insert contains 600 nt upstream of the start codon, the complete coding sequence and 101 nt downstream from stop codon. All three *rne* promoters and its terminator are included within the insert. The empty vector, pWSK129, lacks this insert and only contains the pQLK26 backbone with a single Sall site.

We were unable to make mutations in pSG-Rne using the “Quikchange” method (Stratagene, Inc.), possibly due to its length. To solve this problem we divided the 3,881 bp insert described above into two fragments, Rne-frag 1 and Rne-frag 2, and then subcloned them into pUC19 (Step 2; see Table 1 for primers). Rne-frag 1 is 1157 bp long and spans the 5' *Sall* site 600 bp upstream of the *rne* start codon to the single *HindIII* site in the *rne* gene. Rne-frag 2 (2742 bp) begins at the same *HindIII* site and extends past the stop codon to the 3' *Sall* site. Both fragments were amplified from pSG-Rne using the appropriate primers in Table 1 and then inserted separately into pUC19. Initially, all clones of Rne-frag2 in pUC19 contained mutations creating early stop codons, possibly because Rne-frag2 would be in-frame with the *lacZ* fragment in the vector. Presumably the *lacZ-rne* fragment was being expressed and was toxic. To avoid this, an *EcoRI* site was added upstream and adjacent to the *HindIII* site of Rne-frag2 (primer *rne-5'-HindIII* F) so that the 1157 bp fragment was placed in the opposite sense to the *lacZ* fragment in pUC19. The cloning of these two fragments of *rne* into pUC19 created two new plasmids, pUC19-Rnefrag1 and pUC19-Rnefrag2 (Step 2, B).

The two *rne* fragments were mutated in two steps using overlap primer extension (Step 3; see Supplementary Table 2 for primers). Mutations R169Q, T170A, F57A, and F67A were made using pUC19-Rne frag 1 as template. Digestion with *HindIII* and *Sall* and ligation into pUC19 created mutant plasmids pUC19-RneR169Q, pUC19-RneT170A, pUC19-RneF57A, and pUC19-RneF67A respectively. Mutations D303A, D346A, R337Q and R337E were made using pUC19-Rne frag 2 as template resulting in plasmids pUC19-RneD303A, pUC19-RneD346A, pUC19-RneR337Q, and pUC19-RneR337E respectively.

Fragments containing mutations of interest were released from the pUC19 backbone with *Sal I* and *Hind III*, purified and ligated into pWSK129 cleaved with *Sall* along with the wild type Rne fragment needed to make a full length insert (Step 4). Three part ligations were performed using the Rapid DNA Ligation Kit (Roche) using the following combinations.

1. For R169Q, T170A, F57A, and F67A (to create pSG-RneR169Q, pSG-RneT170A, pSG-RneF57A, and pSG-RneF67A): (a) mutant Rne-frag1 (*Sall/HindIII*) plus (b) wild type Rne-frag2 (*HindIII/Sall*) plus (c) pWSK129 backbone (*Sall/Sall*).
2. For D303A, D346A, R337Q, and R337E (to create pSG-RneD303A, pSG-RneD346A, pSG-RneR337Q, and pSG-RneR337E): (a) wild type Rne-frag1 (*Sall/HindIII*) plus (b) mutant Rne-frag2 (*Sall/HindIII*) plus (c) pWSK129 backbone (*Sall/Sall*).

SUPPLEMENTARY FIGURE 2. Purification of an RNase G mutant. Preparation of mutant enzymes was performed as described in Experimental Procedures and ref. 2. Samples containing 2-25 µg protein were separated by SDS-gel electrophoresis and visualized by staining with Coomassie brilliant blue. Panel A shows the early steps in the purification of RNase G R171Q. Lane 1, markers (relative masses indicated in the right margin); lane 2, flow through from the Talon ® column; lane 3, material eluted with a high salt wash; lane 4, sample of the material adsorbed to the Talon resin; lane 5, material eluted with 50 mM Tris-HCl, pH 7.6 + 50 mM NaCl; lane 6, material eluted in the same buffer containing 10 mM imidazole; lane 7, material eluted in the same buffer with 50 mM imidazole; lane 8, material eluted with the same buffer containing 500 mM imidazole. Panel B shows the elution of RNase G R171Q from a Source Q column. Lane M contains molecular mass markers; material in lanes 11-12 was pooled for assays.

REFERENCES

1. Ow, M.C., Liu, Q., and Kushner, S.R. (2000) *Mol. Microbiol.* **38**, 854-865.
2. Briant, D.J., Hankins, J.S., Cook, M.A., and Mackie, G.A. (2003) *Mol. Microbiol.* **50**, 1381-1390.

Supplementary Table 1. Oligonucleotide primers for amplifying and subcloning RNase E mutants

Name/Purpose	Sequence
<i>rne</i> -5' forward ^a	5'-TTTAT <i>GTTCGACCGGATGGAGTCTCTGTTTTTCATGGTTGGC</i>
<i>rne</i> -3' reverse ^a	5'-TTTAT <i>GTTCGACGGTTAGCAAGGATGCCATTTCGATG</i>
<i>rne</i> -5'- <i>HindIII</i> F ^b	5'-AAAGAATTCAAGCTTCCGTCTGAAACACTGG
<i>rne</i> -3'- <i>HindIII</i> R ^c	5'-CCCAGTGTTTCAGACGGAAGCTTAAATCCCATTGCAGCGCCTCAGC
Rne pET24b F ^d	5'-GAAGGAGATATACATATGAAAAGAATGTTAAT CAACGCAACTC
Rne pET24b R ^d	5'-GTGGTGCTCGAGCAGCGCAGGTTGTTCCGGACGCTTA CGTTCAGCG

a. Primers for the amplification of the 3,881bp fragment encompassing the *rne* gene and containing *SalI* sites (italicized) for ligation into pWSK129.

b. Primer for amplification of Rne frag 2 (see Suppl. Fig. 1)

c. Reverse primer for amplification of Rne frag 1 (see Suppl. Fig. 1)

d. Primers for amplification of the coding sequence for (amino acid) residues 1-529 from RNase E.

Supplementary Table 2. Oligonucleotide primers for construction of RNase E mutants

Mutation	Oligonucleotides
F57A	5'-GGCATTAGTTGTCGTCGTCGAAGGTCTG 5'-CCGTAATCAACAGCAGCAGCTTCCAGAC
F67A	5'-GAACGTCACGGTGCCCTCCCACTAAAAG 5'-CTTTTAGTGGGAGGGCACCGTGACGTTC
R169Q ^a	5'-CGGAAGCTTAAATCCCATTGCAGCGCCTCAGCAGATTTGCCGACG- CCAGCGGTTTGCACGATAAGCCC
T170A ^a	5'-CGGAAGCTTAAATCCCATTGCAGCGCCTCAGCAGATTTGCCGACG- CCAGCGGCGCGCACGATAAG
D303A	5'-CGTTAACGGCCATCGCCATCAACTCCGC 5'-GCGGAGTTGATGGCGATGGCCGTTAACG
R337E	5'-GCTCGTCAGCTGCGCCTGGAAGACCTCGGCGGCCTGATTG 5'-CAATCAGGCCCGCCGAGGTCTTCCAGGCGCAGCTGACGAGC
R337Q	5'-CAGCTGCGCCTGCAAGACCTCGGCGGCCTG 5'-CAGGCCCGCCGAGGTCTTGCAGGCGCAGCTG
D346A	5'-CCTGATTGTTATCGCCTTCATCGACAT 5'-CATGTCGATGAAGGCGATAACAATCA

a. Because the site of mutation was close to the 3'-end of Rne-frag 1, a single primer sufficed for both mutagenesis and primer extension.

Supplementary Table 3.

Oligonucleotide primers for construction of RNase G mutants

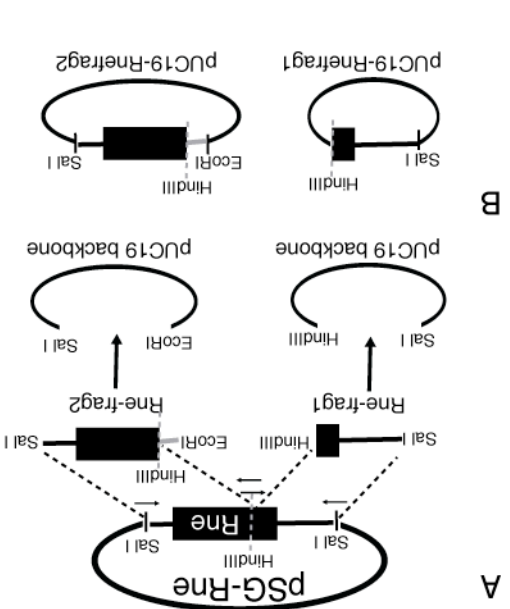
Mutation ^a	Oligonucleotides ^b
F57A	5'-GTATGCAGGCGGCGCATGTAGATATTGG 5'-CCAATATCTACATGCGCCGCCTGCATAC
F67A	5'-TGGATAAAGCCGCGCACTTCATGCATCC 5'-GGATGCATGAAGTGCCGCGGCTTTATCCA
K115A	5'-ATGGTGCAGGTGGTGGCAGATCCGCTTG 5'-CAAGCGGATCTGCCACCACCTGCACCAT
V131I	5'-CCTTCTCGCTATCTGATCTTTATGCCAGGGGC 5'-GCCCCTGGCATAAAGATCAGATAGCGAGAAGG
R171H	5'-GGGTTTATCATCCATACCGCAGCGGAAG 5'-CTTCCGCTGCGGTAIGGATGATAAACCC
R171Q	5'-GGCGGGTTTATCATCCAAACCGCAGCGGAAGGG 5'-CCCTTCCGCTGCGGTTIGGATGATAAACCCGCC
E298A	5'-ATCGACCAGACCGCAGCGATGACCACC 5'-GGTGGTCATCGCTGCGGTCTGGTCGATAATG
D304A	5'-GATGACCACCGTGGCCATCAAATACCGGAG 5'-CTCCGGTATTGATGGCCACGGTGGTCATC
E326A	5'-CCATTTTCAATACCAATATTGCAGCGACGCAGGCTATC 5'-GATAGCCTGCGTCGCTGCAATATTGGTATTGAAAATGG
R338Q	5'-GCTCGCCAGTTACGGTTGCAAAATCTGGGCGGGATTATC 5'-GATAATCCCGCCCAGATTTIGCAACCGTAACTGGCGAGC
D347A	5'-GGCGGGATTATCATTATTGCTTTCATCGATATGAATAATGAAG 5'-CTTCATTATTCATATCGATGAAAGCAATAATGATAATCCCGCC
D350A	5'-CATTATTGATTTTCATCGCTATGAATAATGAAGATCACCGCC 5'-GGCGGTGATCTTCATTATTCATAGCGATGAAATCAATAATG

a. Amino acids are numbered from the Met in the sequence, MTAELL... , which has been shown to be the natural N-terminus (2).

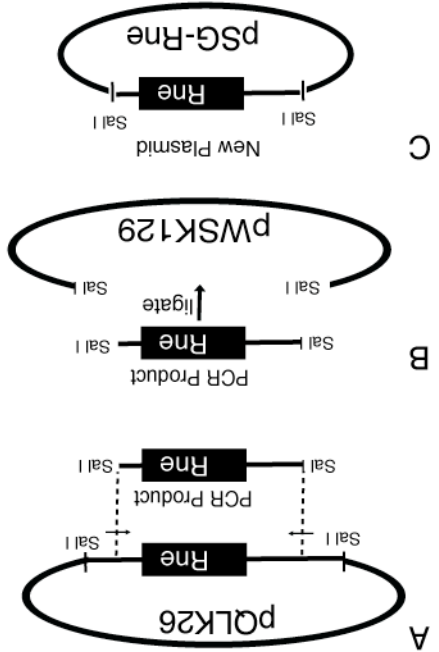
b. Residues at the site of mutation are underlined.

Suppl. Fig. 1

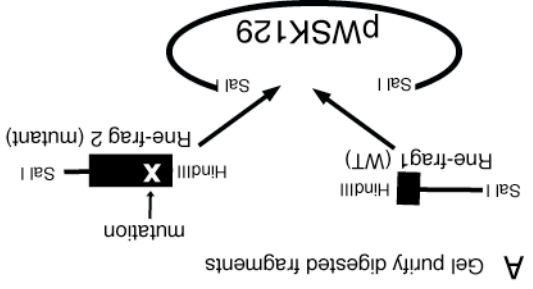
Step 2: Divide insert into two pieces and subclone into pUC19



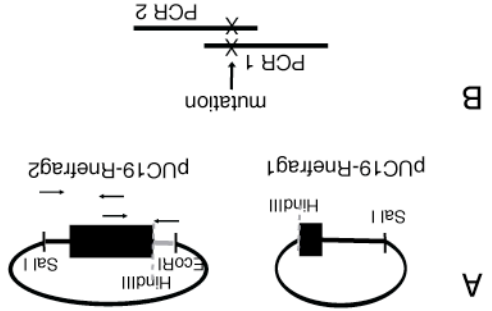
Step 1: Shorten Rne insert



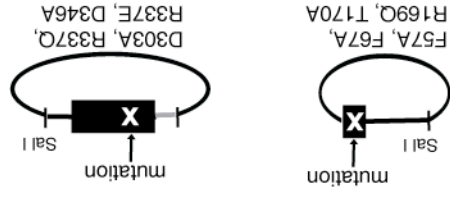
Step 4: Move mutation back into pWSK129 with a three piece ligation



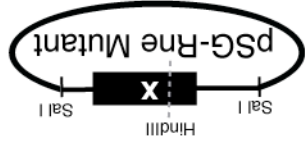
Step 3: Mutate Rne in pUC19



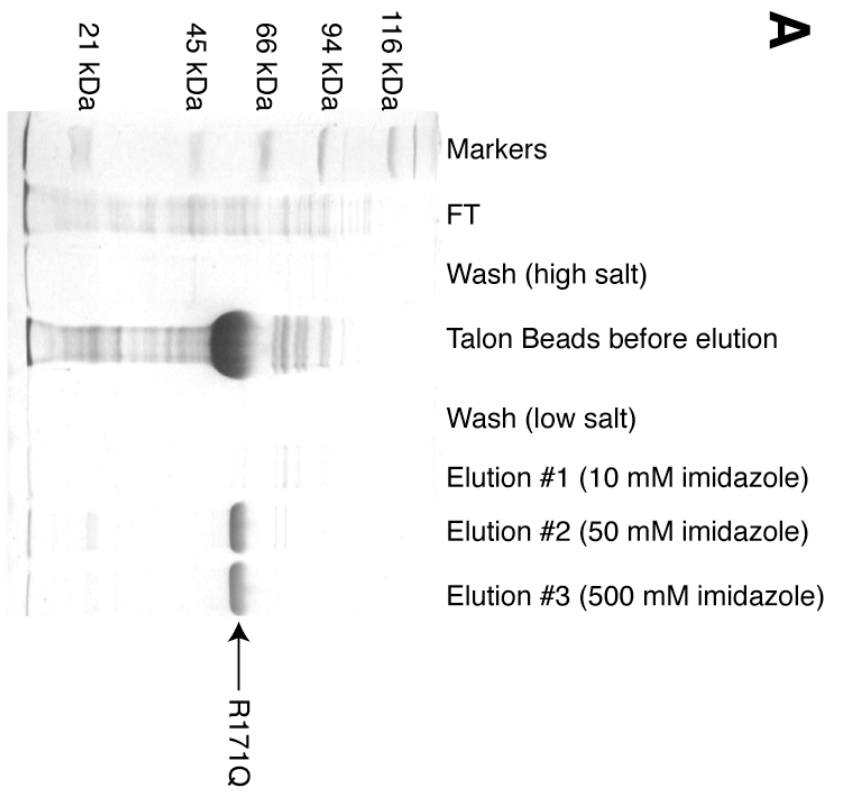
D New plasmids with mutated fragments in pUC19



C New plasmid with full length Rne E and mutation



A



Suppl. Fig. 2

B

